Supplement for

- 2 An improved GRACE-derived groundwater storage
- anomaly (igGWSA) dataset over global land with full
- 4 consideration of non-groundwater components based on
- 5 current new datasets
- 6 Zongxia Wang^{a, b}, Suxia Liu^{a, b, c}, Xingguo Mo^{a, b, c}
- ^a Key Laboratory of Water Cycle and Related Land Surface Processes, Institute of Geographic Sciences
- 8 and Natural Resources Research, Chinese Academy of Sciences, Beijing 100101, China
- 9 b College of Resources and Environment, University of Chinese Academy of Sciences, Beijing 100049,
- 10 China
- 11 ° Sino-Danish College, University of Chinese Academy of Sciences, Beijing 100049, China
- 12 *Correspondence to*: Suxia Liu (liusx@igsnrr.ac.cn)

13

1

- 14 Text S1. Methods for estimating glacier water storage
- 15 To be consistent with TWSA data, changes in glacier volume, dvol, can be converted into changes in
- glacier water storage represented as equivalent water height (EWH), dEWH, through Eq. (S1):

$$17 dEWH = \frac{dvol \times \rho_i}{A} , (S1)$$

- where ρ_i and A refer to the density of ice and the area of pixel, respectively. The units for dvol, ρ_i ,
- 19 A, and dEWH are m³, kg/m³, m², and kg/m² (equiv. to mm), respectively.

- 21 Text S2. Methods for estimating permafrost water storage
- 22 Changes in permafrost water storage, ΔPM , can be indirectly estimated from changes in active layer
- thickness (ALT), $\triangle ALT$, by applying Eq. (S2) (Xiang et al., 2016; Zou et al., 2022).

24
$$\Delta PM = -\Delta ALT \left(\frac{(1-n)k\rho_i}{(1-k)\rho_w} - \varepsilon \right) , \tag{S2}$$

- 25 where n is the porosity of soil and rock in the bottom of active layer and is set to 0.4352 m³/m³ (same
- as soil porosity of perennial land ice defined in JRA-55); ρ_i and ρ_w are the density of ice and water,

27 respectively; k is the ice content in the permafrost with an upper limit of 20% (Zhang et al., 2008); ε

28 is the residual water content in the increased active layer and is determined to be 7.93% (Gouttevin et

29 al., 2012).

30

31

Text S3. Methods for estimating pixel-wise lake and reservoir water storage

- 32 The temporal resolution of GLWS is near-monthly and was resampled to monthly by using linear
- 33 interpolation. The water storage data are archived lake by lake instead of grid by grid. To allow for
- 34 spatial analysis, we first identified the geographical locations of all grids intersecting with a given lake
- 35 or reservoir at a 0.5° × 0.5° resolution based on the vector boundaries derived from HydroLAKES
- dataset. Next, pixel-wise water storage for the given lake or reservoir can be obtained through Eq. (S3).

$$V_i = V_{total} \times \frac{A_i}{A_{total}}, \tag{S3}$$

- 38 where V_{total} and A_{total} are the total water storage and area of the lake or reservoir, respectively; V_i
- 39 and A_i are the allocated water storage and intersecting area of the *i*th grid, respectively.

40

41

Text S4. Data processing of multi-source RZSM simulations

- 42 The stratification of root zone is 0–100 cm for GLDAS CLSM and MERRA-2; 0–10 cm, 10–40 cm,
- 43 and 40-100 cm for GLDAS Noah and FLDAS Noah; and 0-7 cm, 7-28 cm, and 28-100 cm for
- ERA5-Land. In terms of unit, RZSM is represented as water storage (kg/m², equiv. to mm) in GLDAS
- Noah and GLDAS CLSM, volumetric water content (m³/m³) in FLDAS Noah and ERA5-Land, and
- 46 relative moisture (%) in MERRA-2. To be comparable with PSM, RZSM should be quantified by water
- 47 storage consistently. To this end, RZSM for GLDAS Noah and GLDAS CLSM was determined as the
- 48 summation of water storage in different layers. As for FLDAS Noah and ERA5-Land, RZSM can be
- obtained through Eq. (S4) with FLDAS Noah as an example.

$$50 RZSM_{FLDAS} = \sum_{k=1}^{K} \theta_k \times d_k , (S4)$$

- where θ_k and d_k are the volumetric water content and thickness of the kth layer, respectively. K is
- 52 the total number of soil layers. As for MERRA-2, relative soil moisture RM should first be converted
- into volumetric water content by multiplying by soil porosity p derived from CLSM. $RZSM_{MERRA-2}$

- was then calculated as the product of volumetric water content and root zone depth (100 cm), as shown
- 55 in Eq. (S5).

$$RZSM_{MERRA-2} = RM \times p \times 100 , \qquad (S5)$$

- 58 Text S5. Methods for obtaining ensemble estimation through BTCH
- Taking RZSM as an example, the ensemble estimation $RZSM_{Ensemble}$ can be obtained through Eq.
- 60 (S6) and Eq. (S7).

61
$$RZSM_{Ensemble} = w_1 \times RZSM_1 + w_2 \times RZSM_2 + \dots + w_N \times RZSM_N$$
, (S6)

62
$$w_n = \frac{\prod_{l=1, l \neq n}^{N} \sigma_l^2}{\sum_{n=1}^{N} (\prod_{l=1, l \neq n}^{N} \sigma_l^2)} ,$$
 (S7)

- where N is the total number of datasets to be integrated (N=5 for RZSM); w_n is the weight of the
- nth dataset; σ_i is the error variance of the *i*th dataset.

65

66 Text S6. Evaluation metrics of RF models

67
$$R^{2} = 1 - \frac{\sum_{i=1}^{N} (PSM_{obs_i} - PSM_{pre_i})^{2}}{\sum_{i=1}^{N} (PSM_{obs_i} - \overline{PSM_{obs}})^{2}},$$
 (S8)

$$RMSE = \sqrt{\frac{1}{N} \sum_{i=1}^{N} \left(PSM_{obs_i} - PSM_{pre_i} \right)^2} , \qquad (S9)$$

$$69 rRMSE = \frac{RMSE}{PSM_0hs} \times 100\% , (S10)$$

- where PSM_{obs_i} is the *i*th PSM value simulated by CLSM; PSM_{pre_i} is the *i*th PSM value predicted
- 71 by RF; $\overline{PSM_{obs}}$ is the average of all PSM_{obs_i} . Higher R² and lower rRMSE indicate greater
- 72 explanatory power and accuracy of the RF model.

73

- Text S7. Component contribution ratio
- 75 To quantify the contribution of a given individual storage component to the interannual variability of
- 76 TWS, the component contribution ratio (CCR) proposed by Kim et al. (2009) was employed, as shown
- 77 in Eq. (S11) and Eq. (S12).

78
$$MAD_S = \frac{1}{N} \sum_{t=1}^{N} |S_t - \bar{S}|$$
, (S11)

79
$$CCR_S = \frac{MAD_S}{\sum_{S=1}^{M} MAD_S} \times 100\%$$
, (S12)

- 80 where MAD_S denotes the mean absolute deviation (MAD) of an individual storage component S (e.g.,
- canopy water storage); \bar{S} is the long-term mean of S during the study period; N is the number of
- 82 years; M is the number of storage components.

Table S1. Consideration of non-groundwater components in previous studies.

Reference	Study area	glaciers	permafrost	lakes and	surface	snow	canopy	soil
				reservoirs	runoff		water	moisture
Yi et al. (2016)	China	×	×	×	×	×	×	✓
Lv et al. (2021)	China	×	×	×	×	✓	✓	✓
Zhao et al. (2023)	China	×	×	×	×	✓	✓	✓
Lin et al. (2020)	Lhasa River Basin	×	×	×	×	✓	×	✓
Zhu and Zhang (2022)	Yangtze River Basin, Yellow River Basin	×	×	×	×	✓	✓	✓
Liu et al. (2023)	northwest China	×	×	✓	✓	✓	✓	✓
Peng et al. (2021)	Central Asia	×	×	×	×	✓	\checkmark	✓
Forootan et al. (2017)	the Middle East	×	×	✓	×	✓	✓	✓
Nikraftar et al. (2024)	the Middle East	×	×	×	✓	✓	×	✓
Shin et al. (2021)	Nepal	×	×	×	✓	✓	✓	✓
Montecino et al. (2016)	Northern Chile	×	×	×	×	✓	×	✓
Sproles et al. (2015)	Canada	×	×	✓	×	✓	×	✓
Zhu et al. (2022)	Canada	×	×	×	×	✓	×	✓

Table S1 (continued). Consideration of non-groundwater components in previous studies.

Reference	Study area	glaciers	permafrost	lakes and	surface	snow	canopy	soil
				reservoirs	runoff		water	moisture
Muskett and Romanovsky (2011)	Alaska	×	×	×	√	×	×	×
Wang et al. (2022)	North America	×	×	✓	×	✓	×	✓
Xanke and Liesch (2022)	Euro-Mediterranean region	×	×	×	✓	✓	×	✓
Muskett and Romanovsky (2009)	Arctic	×	×	×	✓	×	×	×
Lin et al. (2022)	Arctic	×	×	×	✓	✓	×	✓
Jin and Feng (2013)	Global	×	×	×	✓	✓	✓	✓
Xiang et al. (2016)	Tibetan Plateau	✓	✓	✓	×	\checkmark	×	✓
Zhang et al. (2017)	Tibetan Plateau	✓	✓	✓	×	✓	×	✓
Zou et al. (2022)	Tibetan Plateau	✓	\checkmark	✓	×	✓	×	✓
Fan et al. (2023)	northern Himalayas	✓	\checkmark	✓	×	✓	×	✓
Li et al. (2023)	China	✓	×	✓	✓	✓	✓	✓
Liu et al. (2020)	Asia and eastern Europe	✓	×	✓	×	✓	✓	✓
Wang et al. (2018)	global endorheic basins	✓	×	✓	×	✓	✓	✓

Table S2. Interannual trends in igGWSA, $GWSA_{ignored}$, and GlacierWSA in glacier-covered regions.

Region	igGWSA	$GWSA_{ignored} \\$	GlacierWSA	Region	igGWSA	$GWSA_{ignored} \\$	GlacierWSA
Global	-0.19**	-4.03**	-3.85**	Region 10	0.58**	0.30**	-0.28**
Region 1	4.92**	-8.87**	-13.79**	Region 11	1.40**	-0.07	-1.47**
Region 2	1.41**	0.04	-1.36**	Region 12	-0.04	-0.64**	-0.60**
Region 3	3.28**	-10.01**	-13.30**	Region 13	0.32**	-0.35**	-0.66**
Region 4	4.99**	-8.82**	-13.81**	Region 14	0.63**	-0.61**	-1.24**
Region 5	-18.79**	-24.72**	-5.92**	Region 15	0.58**	-1.53**	-2.10**
Region 6	12.49**	-7.78**	-20.27**	Region 16	0.37**	0.08	-0.29**
Region 7	7.86**	-7.16**	-15.03**	Region 17	2.25**	-2.37**	-4.62**
Region 8	1.73**	0.47*	-1.27**	Region 18	1.54**	0.15	-1.38**
Region 9	-1.42	-10.36**	-8.95**				

Note: Unit: cm/yr. * indicates significance at the 0.05 level. ** indicates significance at the 0.01 level.

Table S3. Interannual trends in igGWSA, GWSA $_{simplified}$, and LRWSA in giant lakes.

Lake	igGWSA	$GWSA_{simplified}$	LRWSA	Lake	igGWSA	$GWSA_{simplified}$	LRWSA
Global	-0.19**	-0.35**	-0.11	Malawi	2.60**	-1.32**	-3.92**
Caspian Sea	0.77*	-4.82**	-5.58**	Great Slave	-0.66*	-0.74**	-0.09
Great Lakes of NA	-1.74*	0.99**	2.72**	Winnipeg	-0.30	0.68**	0.98
Victoria	-1.45	1.56*	3.01**	Ladoga	-0.78	0.39*	1.17
Tanganyika	-0.53	0.39	0.92	Balkhash	-1.40*	-0.04	1.36*
Baikal	0.68**	-0.70**	-1.38**	Aral Sea	11.46**	-1.15**	-12.60**
Great Bear	-0.09	-0.13**	-0.03	Lakes of Tibetan Plateau	-2.31**	0.04	2.62**

Note: Unit: cm/yr. * indicates significance at the 0.05 level. ** indicates significance at the 0.01 level.

Table S4. Interannual trends in igGWSA, GWSA₂₀₀, and GWSA₂₈₉ in deep-soil areas.

Region	igGWSA	GWSA_{200}	GWSA_{289}	Region	igGWSA	GWSA_{200}	GWSA ₂₈₉
Mississippi	-0.08	-0.08	-0.03	Congo	0.06	-0.24**	0.53**
Volga	-0.24*	-0.37**	-0.16**	Songhua-Liaohe	-0.06	-0.07	0.39*
Ob	0.03	-0.06	0.22**	Pampas	-0.08	-0.16	0.69**
Loess Plateau	-0.83**	-0.99**	-0.42**	Ganges-Brahmaputra	-1.09**	-1.25**	-1.24**

Note: Unit: cm/yr. * indicates significance at the 0.05 level. ** indicates significance at the 0.01 level.

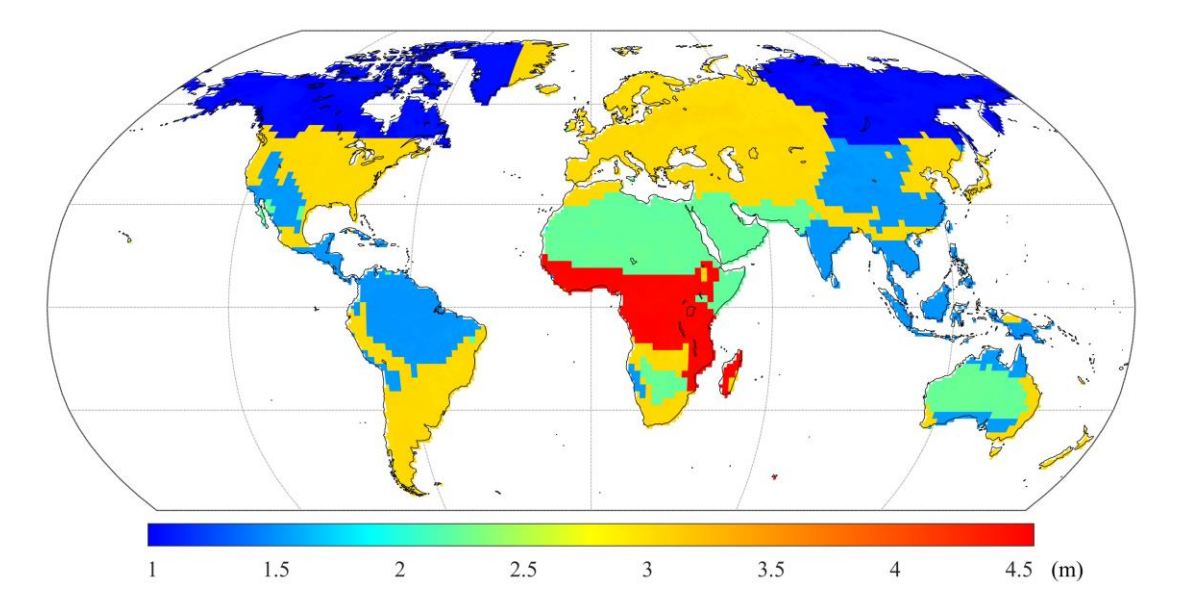


Figure S1. Soil depth information defined in GLDAS VIC model.

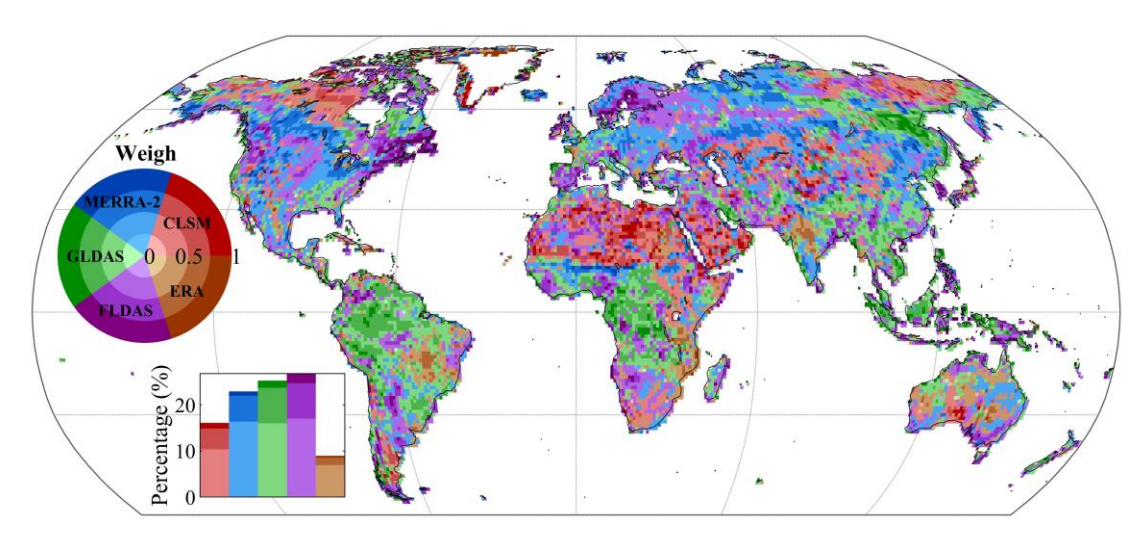


Figure S2. Map of the optimal RZSM dataset.

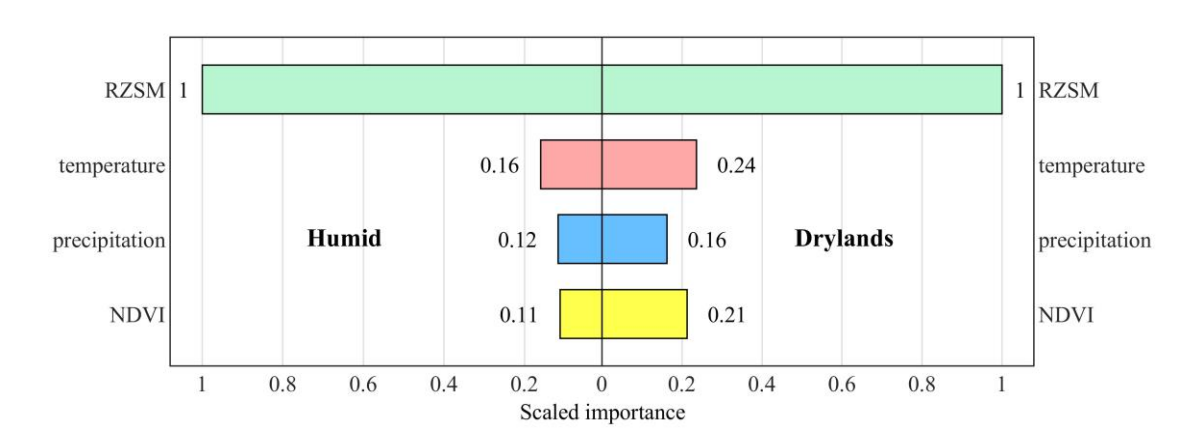


Figure S3. Scaled importance of predictor variables for PSM modelling in humid regions and drylands.

Note: Scaled importance was derived by setting the value of RZSM to 1 and proportionally scaling the values of other variables.



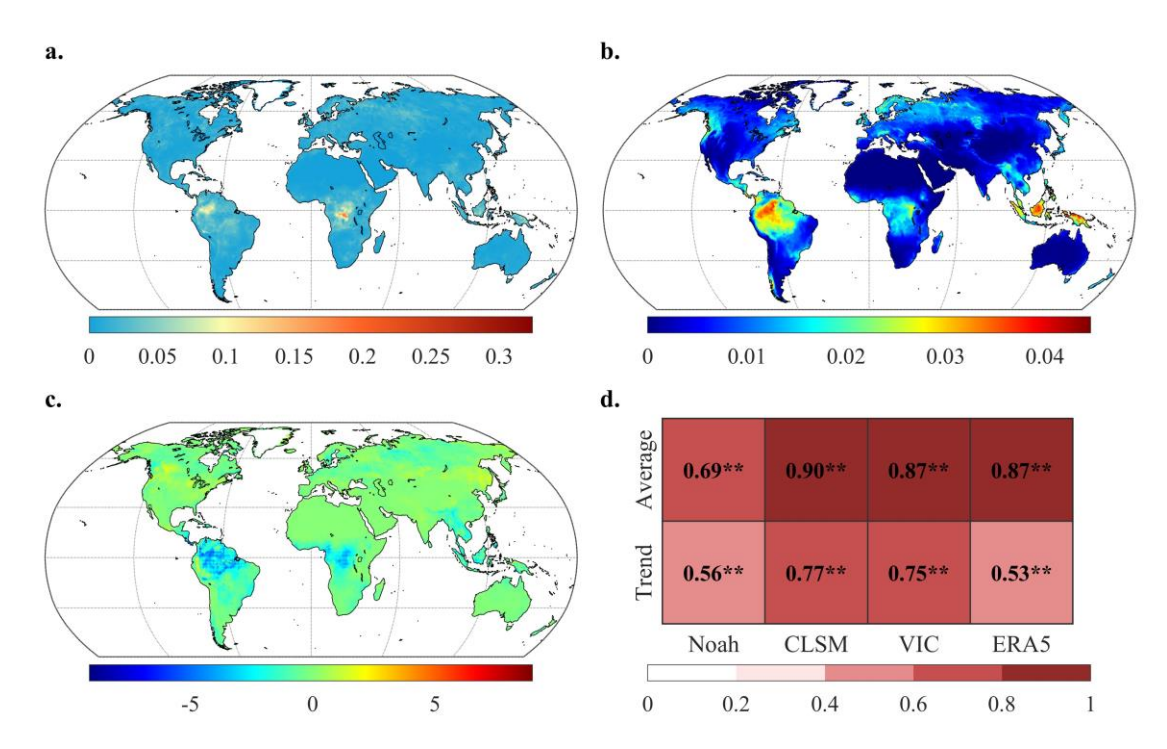


Figure S4. (a) Map of contribution ratio of canopy water storage (CWS) to TWS variability (unit: %). (b)

Map of the multi-year (2000–2019) average of CWS (unit: cm). (c) Map of the interannual trend in CWS (unit: e-04 cm/yr). The three maps consistently revealed that the hotspots of CWS variability were located in tropical rainforest regions, encompassing the Amazon Basin, the Congo Basin, and Southeast Asia. The three maps were made based on the ensemble data of CWS simulations from four LSMs, i.e., GLDAS Noah, GLDAS CLSM, GLDAS VIC, and ERA5-Land. (d) The spatial Pearson's correlation coefficients between the four single-source data and the ensemble data for both multi-year average and interannual trend. ** indicates significance at the 0.01 level. The spatiotemporal patterns of CWS revealed by the four single-source data were all highly consistent with the ensemble data, indicating the high robustness of map a, b, and c.

References

Fan, L., Kuang, X., Or, D., and Zheng, C.: Streamflow composition and water "imbalance" in the Northern Himalayas, Water Resour. Res., 59, e2022WR034243,

- 125 https://doi.org/10.1029/2022wr034243, 2023.
- Forootan, E., Safari, A., Mostafaie, A., Schumacher, M., Delavar, M., and Awange, J. L.: Large-scale
- 127 total water storage and water flux changes over the arid and semiarid parts of the Middle East from
- 128 GRACE and reanalysis products, Surv. Geophys., 38, 591-615,
- 129 https://doi.org/10.1007/s10712-016-9403-1, 2017.
- Gouttevin, I., Krinner, G., Ciais, P., Polcher, J., and Legout, C.: Multi-scale validation of a new soil
- freezing scheme for a land-surface model with physically-based hydrology, Cryosphere, 6, 407-430,
- https://doi.org/10.5194/tc-6-407-2012, 2012.
- 133 Jin, S. and Feng, G.: Large-scale variations of global groundwater from satellite gravimetry and
- hydrological models, 2002-2012, Global Planet. Change, 106, 20-30,
- https://doi.org/10.1016/j.gloplacha.2013.02.008, 2013.
- 136 Kim, H., Yeh, P. J. F., Oki, T., and Kanae, S.: Role of rivers in the seasonal variations of terrestrial
- 137 water storage over global basins, Geophys. Res. Lett., 36, L17402,
- https://doi.org/10.1029/2009g1039006, 2009.
- Li, Q., Pan, Y., Zhang, C., and Gong, H.: Quantifying multi-source uncertainties in GRACE-based
- estimates of groundwater storage changes in mainland China, Remote Sens., 15, 2744,
- 141 https://doi.org/10.3390/rs15112744, 2023.
- Lin, H., Cheng, X., Zheng, L., Peng, X., Feng, W., and Peng, F.: Recent changes in groundwater and
- surface water in large Pan-Arctic river basins, Remote Sens., 14, 607,
- 144 https://doi.org/10.3390/rs14030607, 2022.
- Lin, L., Gao, M., Liu, J., Wang, J., Wang, S., Chen, X., and Liu, H.: Understanding the effects of
- climate warming on streamflow and active groundwater storage in an alpine catchment: the upper
- Lhasa River, Hydrol. Earth Syst. Sci., 24, 1145-1157, https://doi.org/10.5194/hess-24-1145-2020,
- 148 2020.
- Liu, Q., Xu, Y., Chen, J., and Cheng, X.: Multi-source satellite reveals the heterogeneity in water
- storage change over northwestern China in recent decades, J. Hydrol., 624, 129953,
- 151 https://doi.org/10.1016/j.jhydrol.2023.129953, 2023.
- Liu, X., Feng, X., Ciais, P., and Fu, B.: Widespread decline in terrestrial water storage and its link to
- teleconnections across Asia and eastern Europe, Hydrol. Earth Syst. Sci., 24, 3663-3676,

- https://doi.org/10.5194/hess-24-3663-2020, 2020.
- Lv, M., Ma, Z., and Yuan, N.: Attributing terrestrial water storage variations across China to changes in
- 156 groundwater and human water use, J. Hydrometeorol., 22, 3-21,
- 157 https://doi.org/10.1175/jhm-d-20-0095.1, 2021.
- Montecino, H. C., Staub, G., Ferreira, V. G., and Parra, L. B.: Monitoring groundwater storage in
- northern Chile based on satellite observations and data simulation, Bol. Cienc. Geod., 22, 1-15,
- 160 https://doi.org/10.1590/s1982-21702016000100001, 2016.
- 161 Muskett, R. R. and Romanovsky, V. E.: Groundwater storage changes in arctic permafrost watersheds
- from GRACE and in situ measurements, Environ. Res. Lett., 4, 045009,
- https://doi.org/10.1088/1748-9326/4/4/045009, 2009.
- 164 Muskett, R. R. and Romanovsky, V. E.: Alaskan permafrost groundwater storage changes derived from
- GRACEand ground measurements, Remote Sens., 3, 378-397, https://doi.org/10.3390/rs3020378,
- 166 2011.
- 167 Nikraftar, Z., Parizi, E., Saber, M., Hosseini, S. M., Ataie-Ashtiani, B., and Simmons, C. T.:
- Groundwater sustainability assessment in the Middle East using GRACE/GRACE-FO data,
- Hydrogeol. J., 32, 321-337, https://doi.org/10.1007/s10040-023-02717-3, 2024.
- Peng, Q., Wang, R., Jiang, Y., Li, C., and Guo, W.: The change of hydrological variables and its effects
- 171 on vegetation in Central Asia, Theor. Appl. Climatol., 146, 741-753,
- https://doi.org/10.1007/s00704-021-03730-w, 2021.
- 173 Shin, S., Pokhrel, Y., Talchabhadel, R., and Panthi, J.: Spatio-temporal dynamics of hydrologic changes
- in the Himalayan river basins of Nepal using high-resolution hydrological-hydrodynamic modeling,
- J. Hydrol., 598, 126209, https://doi.org/10.1016/j.jhydrol.2021.126209, 2021.
- 176 Sproles, E. A., Leibowitz, S. G., Reager, J. T., Wigington, P. J., Jr., Famiglietti, J. S., and Patil, S. D.:
- GRACE storage-runoff hystereses reveal the dynamics of regional watersheds, Hydrol. Earth Syst.
- 178 Sci., 19, 3253-3272, https://doi.org/10.5194/hess-19-3253-2015, 2015.
- Wang, H., Xiang, L., Steffen, H., Wu, P., Jiang, L., Shen, Q., Li, Z., and Hayashi, M.: GRACE-based
- 180 estimates of groundwater variations over North America from 2002 to 2017, Geod. Geodyn., 13,
- 181 11-23, https://doi.org/10.1016/j.geog.2021.10.003, 2022.

- Wang, J., Song, C., Reager, J. T., Yao, F., Famiglietti, J. S., Sheng, Y., MacDonald, G. M., Brun, F.,
- 183 Schmied, H. M., Marston, R. A., and Wada, Y.: Recent global decline in endorheic basin water
- storages, Nat. Geosci., 11, 926-932, https://doi.org/10.1038/s41561-018-0265-7, 2018.
- 185 Xanke, J. and Liesch, T.: Quantification and possible causes of declining groundwater resources in the
- Euro-Mediterranean region from 2003 to 2020, Hydrogeol. J., 30, 379-400,
- 187 https://doi.org/10.1007/s10040-021-02448-3, 2022.
- 188 Xiang, L., Wang, H., Steffen, H., Wu, P., Jia, L., Jiang, L., and Shen, Q.: Groundwater storage changes
- in the Tibetan Plateau and adjacent areas revealed from GRACE satellite gravity data, Earth Planet.
- 190 Sci. Lett., 449, 228-239, https://doi.org/10.1016/j.epsl.2016.06.002, 2016.
- 191 Yi, S., Wang, Q., and Sun, W.: Basin mass dynamic changes in China from GRACE based on a
- multibasin inversion method, J. Geophys. Res.: Solid Earth, 121, 3782-3803,
- 193 https://doi.org/10.1002/2015jb012608, 2016.
- Zhang, G., Yao, T., Shum, C. K., Yi, S., Yang, K., Xie, H., Feng, W., Bolch, T., Wang, L., Behrangi, A.,
- 25 Zhang, H., Wang, W., Xiang, Y., and Yu, J.: Lake volume and groundwater storage variations in
- Tibetan Plateau's endorheic basin, Geophys. Res. Lett., 44, 5550-5560,
- 197 https://doi.org/10.1002/2017gl073773, 2017.
- 28 Zhang, T. J., Barry, R. G., Knowles, K., Heginbottom, J. A., and Brown, J.: Statistics and
- 199 characteristics of permafrost and ground-ice distribution in the Northern Hemisphere, Polar Geogr.,
- 200 31, 47-68, https://doi.org/10.1080/10889370802175895, 2008.
- 201 Zhao, K., Fang, Z., Li, J., and He, C.: Spatial-temporal variations of groundwater storage in China: a
- 202 multiscale analysis based on GRACE data, Resour. Conserv. Recycl., 197, 107088,
- 203 https://doi.org/10.1016/j.resconrec.2023.107088, 2023.
- 204 Zhu, Q. and Zhang, H.: Groundwater drought characteristics and its influencing factors with
- corresponding quantitative contribution over the two largest catchments in China, J. Hydrol., 609,
- 206 127759, https://doi.org/10.1016/j.jhydrol.2022.127759, 2022.
- Zhu, Y., Myint, S. W., Schaffer-Smith, D., Sauchyn, D. J., Xu, X., Piwowar, J. M., and Li, Y.:
- 208 Examining ground and surface water changes in response to environmental variables, land use
- dynamics, and socioeconomic changes in Canada, J. Environ. Manage., 322, 115875,

- 210 https://doi.org/10.1016/j.jenvman.2022.115875, 2022.
- 211 Zou, Y., Kuang, X., Feng, Y., Jiao, J. J., Liu, J., Wang, C., Fan, L., Wang, Q., Chen, J., Ji, F., Yao, Y.,
- and Zheng, C.: Solid water melt dominates the increase of total groundwater storage in the Tibetan
- 213 Plateau, Geophys. Res. Lett., 49, e2022GL100092, https://doi.org/10.1029/2022g1100092, 2022.